ChemComm

Accepted Manuscript

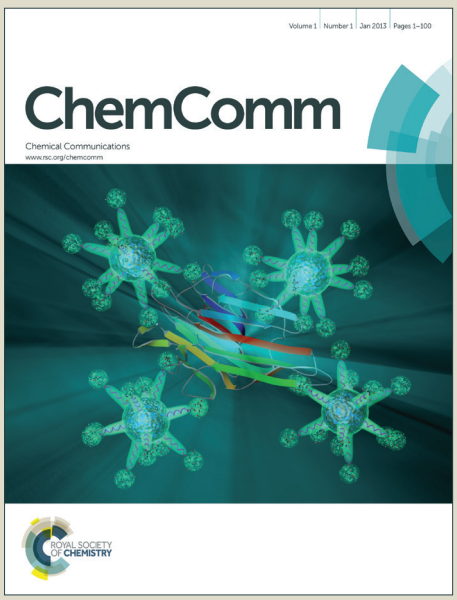

ROYAL SOCIETY OF CHEMISTRY

www.rsc.org/chemcomm

Journal Name

RSCPublishing

COMMUNICATION

Construction of nanoantennas on the bacterial outer membrane

Cite this: DOI: 10.1039/x0xx00000x

Hiroshi Shiigi,*[a] Maho Fukuda,[a] Takatoshi Tono,[a] Kaori Takada,[a] Tomoyuki Okada,[a] Le Quynh Dung,[a] Yu Hatsuoka,[a] Takamasa Kinoshita,[a] Masahiro Takai,[a] Shiho Tokonami,[b] Hidenobu Nakao,[c] Tomoaki Nishino,[a] Yojiro Yamamoto,[a,d] and Tsutomu Nagaoka[a]

Received 00th January 2012,
Accepted 00th January 2012

DOI: 10.1039/x0xx00000x

www.rsc.org/

We demonstrate a simple manipulation of gold nanoparticles that creates a structure-dependent nanometer-scale antenna on the surface of bacteria. Our studies illuminate the concept of the "effective use of light" based on the absorption and emission of light by antennas formed on bacteria.

Pathogenic bacteria, cause widespread hospital-acquired infections and food poisoning, are a major public health problem worldwide. Methods for the rapid detection and identification of pathogenic bacteria in food, clinical, and environmental samples are required to prevent and diagnose infectious diseases.[1] Since nanobioscience is one of the major areas of scientific progress, it should create important advances that benefit human health.

Metal nanoparticles receive considerable attention because of their unique electrical, optical, and chemical properties, which differ from those of bulk metals and depend strongly on their size, shape, and dispersion state.[2] Among them, gold nanoparticles (AuNPs) possess highly dense electrons and high chemical stability, which make them most useful for numerous and diverse applications. Therefore, AuNPs are employed in a broad range of biological applications that involve physical methods such as microscopy and spectroscopy. The biomedical applications of AuNPs include immunogold-labeled antibodies and viruses.[3] AuNPs also produce an enhanced optical field near their surfaces that can be tuned throughout the visible and near-infrared regions of the spectrum by changing particle size, shape, and dispersion state as well as local environmental conditions. The free electrons present on the AuNP surface express a localized surface plasmon resonance (LSPR) involving collective vibrations induced by interactions with visible light. Accordingly, it should be possible to control the LSPR of a nanometer-scaled antenna structure (a concept known as the "effective use of light") through careful assembly of the AuNPs.[4] The introduction of functional groups such as carboxylate and amine on the AuNP surface can be used for a nanometer-sized structure, providing for excellent interactions with biological systems ranging from biological molecules to cells. Therefore, they are important in applications such as imaging and sensing as well as for fabricating electronic devices.[5]

The membranes of Gram-negative bacteria such as *Pseudomonas aeruginosa*, and *Escherichia coli* contain lipopolysaccharides (LPS) that consist of repeating hydrophilic O-antigenic oligosaccharide side chain, a hydrophilic core polysaccharide chain, and a hydrophobic lipid moiety (lipid A) in Fig. 1. Intact bacterial LPS molecules comprise three structural components that are localized to the outer layer of the cell membrane (ESI, Fig. S1a).[6] LPS is an integral component of the cell wall and comprises functional groups such as hydroxyls, phosphates, carboxylates, and amines that extend outward from the body along with polysaccharides. The identities of Gram-negative bacteria can be determined from their surface structure, because they possess different repeated sequences of saccharide subunits. Observation acquired using a zeta-potential analyzer indicates that *P. aeruginosa* possesses a negatively charged surface when dispersed in a wide range of pH (Fig. S1b). This suggests that the negative charge is pre-dominant on the surface of a bacterium due to phosphate, and carboxylate groups compared with amino groups.[7] A bacterium exhibits weak light-scattering intensity due to its cytoplasm, which consists of 80% water. We formed a nanoantenna based on the chemical structures, including phosphates, carboxylates, and amines, in the outer bacterial membrane. To form antennas on the bacterial surface, we focused on AuNPs with characteristic light-scattering properties and interaction sites which were introduced as a protective layer. To develop a single bacterium detection, we evaluated a function of AuNPs as a nanoantenna.

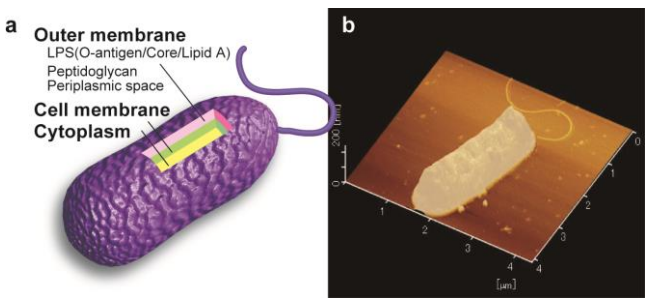

Fig. 1 (a) Schematic of the outer membrane and (b) scanning probe microscopy image of a Gram-negative bacterium (*P. aeruginosa*) using atomic force mode.

AuNPs, which have negative (−24 mV) and positive (+39 mV) charges show a variety of colors from shades of greens to reds in the dark-field images (Fig. S2).[8] Some low-intensity reddish spots, are

typically 1 μm in diameter (a), and high-intensity rod-shaped spots (b) that are 1-μm wide and 2-μm long are observed in Fig. 2A. The intensities were attributed to a red-shift of the LSPRs based on the optical near-field interaction (plasmon coupling) that occurred by aggregation of AuNPs. Kelvin force microscopy (KFM) images revealed different surface potentials of an intact bacterium (Fig. 2B).

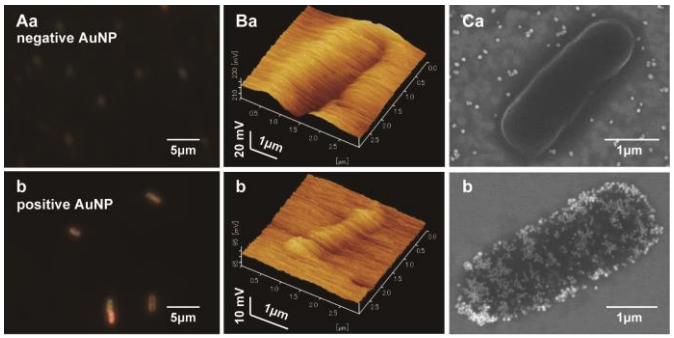

Fig. 2 (A) Dark-field, (B) KFM and (C) SEM images of bacteria with (a) negatively and (b) positively charged AuNPs. The bacterial suspension (9.2×10^8 cells mL^{-1}) was added to the AuNP dispersion (0.028 wt%). An acquisition time of 800 ms was required to obtain dark-field image.

These were confirmed by SEM observations. The negatively charged AuNPs were not observed bound to a bacterium, while the AuNPs along with some aggregates were observed on the Si-wafer substrate (Fig. 2Ca). Therefore, the reddish spots observed in the dark-field image (Fig. 2Aa) was attributable to the AuNPs aggregates without interaction to bacteria on the wafer surface. There was no difference in the potential profiles, depending on the difference of the work function between bacteria and Si-wafer surfaces, among bacteria treated with and without negatively charged AuNPs, since the negative AuNPs did not interact with a bacterium (Fig. 2Ba). As mentioned above, we assume that there was electrostatic repulsion caused by anionic substituents such as phosphate and carboxylate groups present around the amino groups, because a *P. aeruginosa* cell has a negative zeta potential (see Fig. S1). In contrast, almost all of the positively charged AuNPs adsorbed to the bacterial surface and not to the wafer surface, indicating that electrostatic interactions dominated between the AuNPs and the bacterium (Fig. 2Cb). These results indicate that the differences in the dark-field and KFM images were caused by the adsorption of AuNPs to the bacteria. Therefore, the use of AuNPs permits the analysis of the distribution of charge density on the bacteria according to the functional groups in the outer membrane with a resolution of the particle size (~30 nm). We expected that the use of smaller particles would allow us to analyze the surface with a higher resolution based on particle size. However, it was necessary to use AuNPs of sufficient size, because smaller NPs (< 2 nm) degrade the bacterial cell wall.[9]

We next examined in more detail the interaction between the positively charged AuNPs and *P. aeruginosa*. The dispersion of the AuNPs (indicated as +AuNP) yielded a typical UV−vis spectrum with peak intensity at 522 nm, which was attributable to LSPR (Fig. 3A). The color of the AuNP dispersion is wine-red which is specific to the AuNPs. In contrast, P. aeruginosa has no peak intensity in a visible region except for the peak at 260 nm based on the nucleic acids (see Fig. S1c). Addition of 4.6×10^7 cells to the AuNP dispersion changed the color of the solution to purple-blue. The UV−vis spectrum of the mixture exhibited a broad peak at approximately 580 nm that we attributed to the adsorbed AuNPs on a bacterium caused by their electrostatic attraction. Therefore, we predicted that the color of the mixture becomes distinct when the increased number of bacteria causes precipitation. Contrary to our expectations, the color of the mixture changed gradually from purple-blue to wine-red when increased numbers of *P. aeruginosa* were added to the AuNP dispersion. The spectrum of the mixture was similar to that of AuNP, and the absorbance attributed to the LSPR of AuNPs became sharper and more intense with an increase in the number of bacteria, which induced a blue-shift from 580 to 549 nm. This peak shift depends on the dispersion state of the adsorbed AuNPs onto a bacterium and/or the dispersibility of the AuNPs adsorbed bacteria in the solution.

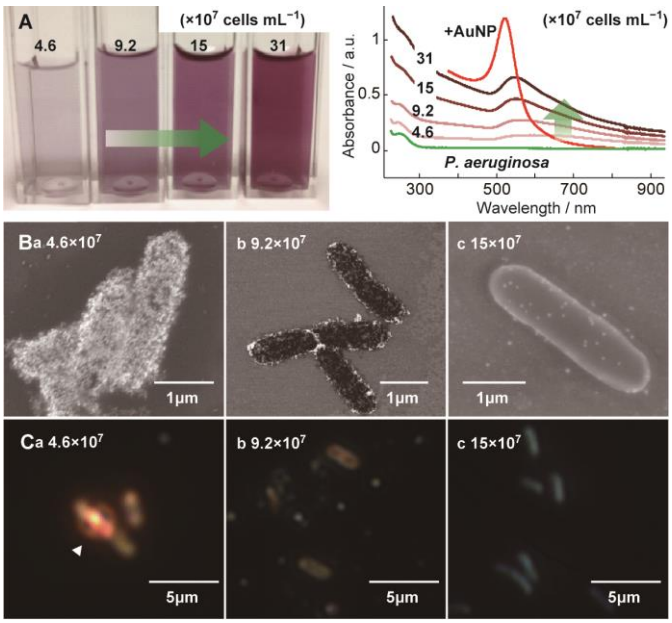

Fig. 3 (A) UV−vis spectra, (B) SEM and (C) dark-field images of the AuNPs adsorbed to bacteria. An acquisition time was 800 ms to obtain dark-field image. The number of bacteria added to the AuNP dispersion is indicated.

SEM revealed a decrease in the number of AuNPs adsorbed to the bacteria when more bacteria were added to the dispersion of AuNPs (Fig. 3B). AuNPs that were tightly adsorbed to the bacteria as well as aggregated bacteria were observed when small numbers of bacteria (4.6×10^7 cells) were added. AuNPs tightly adsorbed to the bacteria generated significant scattering of reddish light due to the plasmon coupling of AuNPs on the bacterium in the dark-field image (Fig. 3Ca). In addition to the plasmon coupling by the AuNPs, strong scattering intensity was caused by overlapping bacteria (shown by an arrow). The positively charged AuNPs adsorbed on a bacterium interacted with a negative surface of other bacterium, causing the bacteria to associate with each other. While the light-scattering intensity of the bacteria became lower with a decrease in the number of adsorbed AuNPs, purplish (b) and greenish colors of bacteria (c) were observed in the dark-field observations (Fig. 3C). These results revealed that the light scattering depended on the amount of AuNPs and their dispersion state on a bacterium. Expression of intensely scattered-light through the plasmon coupling of dense AuNPs that was generated by overlapping bacteria hinted at the effective formation of antennas on a bacterium.

The adsorption of AuNPs on the bacteria generated a significant change in light-scattering properties such as color (wavelength) and strength (intensity). Thus, the excellent light-scattering properties of AuNPs make it possible to use them to build excellent antennas on the bacterial surface. Other metal nanoparticles scatter light intensely and serve as a nanometer-sized index for biological imaging.[10]

However, we chose to use AuNPs because of their chemical stability. Further, metal ions eluted from nanoparticles as well as smaller size are cytotoxic to bacteria and cause the degradation of the outer membrane of dead bacteria.[9,11] Therefore, we used a nanometer-sized raspberry structure with the mean diameter of approximately 100 nm, comprising numerous AuNPs to create a nanoantenna with strong light-scattering property. The nanoraspberry possesses a positive zeta potential of +16.7 mV and a specific structure comprising repeated sequences of AuNP−aniline oligomer−AuNP (Fig. S2), because the aniline oligomer strongly links to adjacent AuNPs with a mean diameter of 5 nm.[12] Therefore, we expected that electrostatic interactions between the raspberries and the bacteria without a destruction of the outer membrane and that strong light scattering would be achieved by the raspberries adsorption.

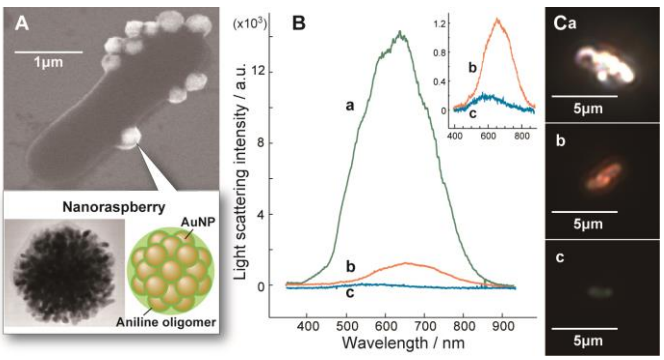

Fig. 4 (A) SEM image of nanoraspberry-labeled bacterium, and (B) light-scattering spectra and (C) dark-field images of the (a) raspberry-, (b) AuNP-, and (c) non-labeled bacteria. The bacterial suspension (3.1×10^7 cells mL^{-1}) was added to the raspberry dispersion (0.038 wt%). Acquisition time was 800 ms.

Although SEM observations revealed only a small amount of nanoraspberries bound to the bacteria (see Fig. 4A), the raspberry-labeled bacterium scattered white-light very strongly (greater by a factor of 10 and 60 compared with a bacterium with and without AuNPs labeling, respectively), as shown in Fig. 4B. Dark-field images show significant differences between raspberries and AuNPs. Although there is a high density of AuNPs in the raspberry, its structure prevents contact between the adjacent AuNPs.[12] Thus, the raspberry emits light with higher intensity through the coupling of LSPR generated by absorption of the incident light.[13] The formation of highly sensitive nanoantennas on a single bacterium was readily accomplished using raspberries.

In summary, we demonstrate here a method for the simple and rapid detection of pathogenic bacteria utilizing AuNPs as a nanoantenna. We successfully and efficiently formed antennas through the electrostatic interaction between the AuNPs and the bacterial outer membrane. The characteristic light-scattering properties of the AuNPs were contributed by their aggregation and dispersion states, which provides useful information regarding the bacteria. To determine in more detail the properties of the outer bacterial membrane that contribute to binding to nanoparticles, it will be necessary to conduct further studies to detect sites of specific molecular recognition using probes for the cell surface, such as antibodies, enzymes and carbohydrate-binding proteins. Moreover, our studies illuminate the concept of the "effective use of light" based on the effective absorption and emission of light by nanoantennas comprised of raspberries, or differentially aggregated AuNPs, or both.

We gratefully acknowledge the financial support provided by the Ministry of Agriculture, Forestry, and Fisheries through a Science and Technology Research Promotion Program for Agriculture, Forestry, Fisheries and Food Industry; and the Japan Society for the Promotion of Science (JSPS) through a Grant-in-Aid for Scientific Research (B) (25288039, 25288069).

Notes and references

[a]Department of Applied Chemistry, and [b]Nanoscience & Nanotechnology Research Center, Osaka Prefecture University, 1-2 Gakuen, Naka, Sakai, Osaka 599-8570, Japan.
[c]National Institute for Materials Science, 1-1 Namiki, Tsukuba, Ibaraki 305-0044, Japan.
[d]GreenChem. Inc., 930-1 Fukuda, Naka, Sakai, Osaka 599-8241, Japan.

† Electronic Supplementary Information (ESI) available: [Experimental procedures and supporting figures]. See DOI: 10.1039/c000000x/

1 (a) P. Daly, T. Collier, S. Doyle, *Lett. Appl. Microbiol.*, 2002, **34**, 222, (b) S. Tokonami, Y. Nakadoi, M. Takahashi, M. Ikemizu, T. Kodama, K. Saimatsu, L. Q. Dung, H. Shiigi, T. Nagaoka, *Anal. Chem*., 2013, **85**, 4925.
2 (a) C. Burda, X. Chen, R. Narayanan, M. A. El-Sayed, *Chem. Rev.*, 2005, **105**, 1025, (b) A. Moores and F. Goettmann, *New J. Chem.*, 2006, **30**, 1121, (c) S. Tokonami, Y. Yamamoto, H. Shiigi, T. Nagaoka, *Anal. Chim. Acta*, 2011, **716**, 76.
3 W. P. Faulk and G. M. Taylor, *Immunochemistry*, 1971, **8**, 1081.
4 (a) A. Moreau, C. Ciracì, J. J. Mock, R. T. Hill, Q. Wang, B. J. Wiley, A. Chilkoti, D. R. Smith, *Nature*, 2012, **492**, 86, (b) G. P. Acuna, F. M. Möller, P. Holzmeister, S. Beater, B. Lalkens, P. Tinnefeld, *Science*, 2012, **338**, 506.
5 (a) D. Porath, A. Bezryadin, S. de Vries, C. Dekker, *Nature*, 2000, **403**, 635, (b) Y. Xiao, F. Patolsky, E. Katz, J. F. Hainfeld, I. Willner, *Science*, 2003, **299**, 1877, (c) H. Shiigi, S. Tokonami, H. Yakabe, T. Nagaoka. *J. Am. Chem. Soc.*, 2005, **27**, 3280, (d) K. Saha, S. S. Agasti, C. Kim, X. Li, V. M. Rotello, *Chem. Rev*., 2012, **112**, 2739.
6 (a) E. T. Rietschel, T. Kirikae, F. U. Schade U. Mamat, G. Schmidt, H. Loppnow, A. J. Ulmer, U. Zähringer, U. Seydel, F. Di Padova, *FASEB J*., 1994, **8**, 217, (b) J. Shephard, A. J. McQuillan, P. J. Bremer, *J. Appl. Environ. Microbiol*., 2008, **74**, 6980.
7 J. B. Fein, C. J. Daughney, N. Yee, T. A. Davis, *Geochim. Cosmochim. Acta*, 1997, **61**, 3319.
8 (a) C. Sönnichsen, T. Franzl, T. Wilk, G. von Plessen, J. Feldmann, O. Wilson, P. Mulvaney, *Phys. Rev. Lett.*, 2002, **88**, 77402, (b) H. Kuwata, H. Tamaru, K. Esumi, K. Miyano, *Appl. Phys. Lett.*, 2003, **83**, 4625, (c) H. Jans, X. Liu, L. Austin, G. Maes, Q. Huo, *Anal. Chem.*, 2009, **81**, 9425.
9 S. C. Hayden, G. Zhao, K. Saha, R. L. Phillips, X. Li, O. R. Miranda, V. M. Rotello, M. A. EI-Sayed, *J. Am. Chem. Soc.*, 2012, **134**, 6920.
10 (a) S. Kyriacou, W. Brownlow, X.-H. N. Xu, *Biochemistry*, 2004, **43**, 140, (b) R. Hu, K.-T. Yong, I. Roy, H. Ding, S. He, P. N. Prasad, *J. Phys. Chem. C*, 2009, **113**, 2676, (c) H. Nakao, S. Tokonami, T. Hamada, H. Shiigi, T. Nagaoka, F. Iwata, Y. Takeda, *Nanoscale*, 2012, **4**, 6814.
11 Z.-m. Xiu, Q.-b. Zhang, H L. Puppala, V. L. Colvin, P. J. J. Alvarez, *Nano Lett*., 2012, **12**, 4271.
12 (a) H. Shiigi, Y. Yamamoto, N. Yoshi, H. Nakao, T. Nagaoka, *Chem. Commun.*, **2006**, 4288, (b) H. Shiigi, R. Morita, Y. Muranaka, S. Tokonami, Y. Yamamoto, H. Nakao, T. Nagaoka, *J. Electrochem. Soc*., 2012, **159**, D442.
13 A. S. Urban, X. Shen, Y. Wang, N. Large, H. Wang, M. W. Knight, P. Nordlander, H. Chen, N. J. Halas, *Nano Lett.*, 2013, **13**, 4399.

Construction of nanoantennas on the bacterial outer membrane

Hiroshi Shiigi, Maho Fukuda, Takatoshi Tono, Kaori Takada, Tomoyuki Okada, Le Quynh Dung, Yu Hatsuoka, Takamasa Kinoshita, Masahiro Takai, Shiho Tokonami, Hidenobu Nakao, Tomoaki Nishino, Yojiro Yamamoto, and Tsutomu Nagaoka

A simple and highly sensitive detection of pathogenic bacteria is available by utilizing gold nanoparticles as an optical antenna.